

# Experimental Stark-broadening studies of the NI multiplet $(^1D)3s^2D - (^1D)3p^2P^o$ at 7904.5 Å

A. Bartecka<sup>a</sup>, T. Wujec, J. Halenka, and J. Musielok

Institute of Physics, Opole University, ul. Oleska 48, 45-052 Opole, Poland

Received 6 October 2003 / Received in final form 23 December 2003

Published online 9 March 2004 – © EDP Sciences, Società Italiana di Fisica, Springer-Verlag 2004

**Abstract.** Experimental Stark-broadening studies of the NI multiplet  $(^1D)3s^2D - (^1D)3p^2P^o$  are reported. Line shape measurements were performed using a wall-stabilized arc operated at atmospheric pressure in helium with small amounts of nitrogen and hydrogen. The radiation of the plasma emitted from nearly homogeneous plasma layers in end-on direction was measured using a grating spectrometer equipped with a charge-coupled device (CCD) detector. The arc current was varied from 35 to 50 A in order to obtain different plasma conditions (electron densities and temperatures). The so-called  $j(x)$  profiles of Griem, convoluted with the corresponding Doppler and apparatus profiles were fitted to the experimental data sets. In this way the Stark broadening parameters: the electron impact shifts ( $d_e$ ) and widths ( $w_e$ ) as well as ion-broadening asymmetry ( $A$ ) for the investigated NI multiplet have been determined.

**PACS.** 32.70.Jz Line shapes, widths, and shifts – 52.70.Kz Optical (ultraviolet, visible, infrared) measurements

## 1 Introduction

Measurements of Stark-broadening and shift parameters of spectral lines provide very useful information applicable for plasma diagnostics. According to the Stark-broadening theory e.g. [1–5], the shapes and shifts of isolated lines of non-hydrogenic neutral atoms are mainly determined by impacts of electrons with radiating atoms, and — to a much smaller extent — by the electric microfields generated by plasma ions. Electron collisions produce a symmetrical and shifted profile of the Lorentzian type, while the ions cause asymmetries as well as contribute somewhat to the width and shift of the profile.

Shapes of spectral lines yield e.g. information on important plasma parameters as the electron density, the heavy particle (gas) temperatures and the radiation transport in stellar atmospheres as well as in technical plasmas. As a consequence of the linear Stark effect, the broadening of spectral lines of hydrogen and hydrogen-like ions play an outstanding role in plasma diagnostics. The widths of hydrogen Balmer lines (especially the  $H_\beta$  line) in the visible part of spectrum are widely used for determination of electron densities in low temperature plasmas. In the case of plasmas where hydrogen is not present or undesirable, non-hydrogenic lines are often applied for diagnostics purposes. In the visible and UV wavelength range

the widths of non-hydrogenic lines are usually significantly smaller in comparison to the widths of lines of the Balmer series. On the other hand the widths of non-hydrogenic transitions depend nearly linearly on electron density, i.e. stronger than the widths of hydrogen transitions. However some particular non-hydrogenic lines exhibit an anomalous strong Stark-broadening and therefore may be very useful in plasma studies. Nitrogen atoms deserve substantial interest in this context, because some NI lines (their widths) may be easily applied as a measure of electron density. Nevertheless broadening, shift and asymmetry data for NI transitions are rather scarce. Therefore in this work we report such investigations for the NI multiplet  $3s^2D - 3p^2P^o$ . This transition, appearing in the red part of the spectrum and exhibiting large spectral intensity, occurs at excited atomic core leading to the parent term  $2s^22p^2(^1D)$ . The anomalous strong broadening of this multiplet has been demonstrated in [6] and the width of one of the fine structure component has been recently calibrated for  $N_e$ -determination [7]. This well isolated multiplet, consists of three fine structure components due to transitions between levels ( $J_l - J_u$ ):  $5/2 - 3/2$ ,  $3/2 - 3/2$ , and  $3/2 - 1/2$ , at wavelengths 7898.98 Å, 7899.28 Å and 7915.42 Å, respectively. The corresponding transition probabilities are  $2.82 \times 10^7 \text{ s}^{-1}$ ,  $3.28 \times 10^6 \text{ s}^{-1}$  and  $3.13 \times 10^7 \text{ s}^{-1}$  [8].

<sup>a</sup> e-mail: bartecka@uni.opole.pl

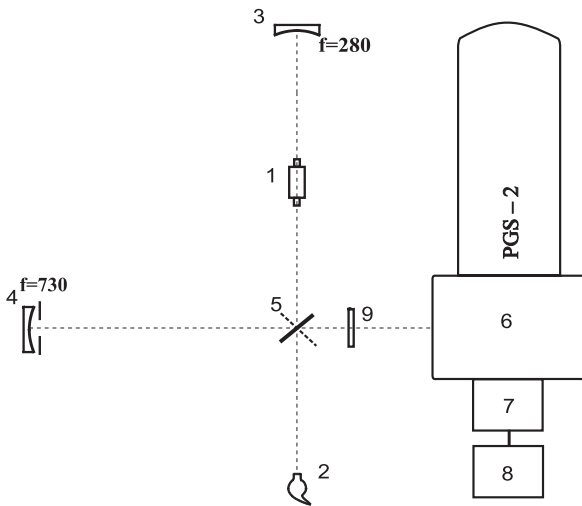


**Fig. 1.** The scheme of the experimental set-up. 1 & 2 – arc and radiometric standard sources; 3 & 4 – concave mirrors; 5 – turnable flat mirror; 6 – spectrometer; 7 – OMA detector; 8 – computer; 9 – spectral filter.

## 2 Experiment

### 2.1 Plasma source and experimental procedure

Our experimental set-up is described in details e.g. in [9,10] therefore we restrict the following discussion to only a few essential remarks being relevant to the present investigation. A wall-stabilized arc with the channel diameter of 4 mm and the length of 70 mm was applied as the excitation source for atomic nitrogen. The arc was operated at atmospheric pressure and at various currents between 35 and 50 amperes. The central part of the arc column was operated in a mixture of helium, nitrogen and hydrogen (93%, 5%, 2% by volume respectively). The regions close to both electrodes were supplied with very small amount of argon in order to improve the stability of the discharge. The arc plasma reveals cylindrical symmetry with rather weak radial electron density and temperature gradients close to the arc axis.

Figure 1 shows the scheme of our experimental set-up. The radiation emerging from the arc (1) was imaged onto the 20  $\mu\text{m}$  wide entrance slit of the grating spectrometer PGS2 (6) using the concave mirror (4) with a large focal length ( $f = 730$  mm). In order to restrict the collection angle of the light emitted from the arc a diaphragm of the diameter of  $\phi = 12$  mm was placed in front of the concave mirror (4). This restriction ensures that only the radiation emitted nearly parallel to the arc axis (homogeneous plasma layers) is forming the arc image on the slit and thus assuring the required resolution in the plane perpendicular to the arc axis. The whole optical imaging system provides conditions for observing radiation originating from well-defined nearly homogeneous plasma layers of the arc column. Measuring the ratio between the FWHM and the peak separation of  $H_{\beta}$  line the homogeneity of individual plasma layers was controlled. The radiation was detected by using a two-dimensional optical multichannel analyzer

OMA4 (7) with regular pixel gaps of 0.019 mm. A reflection grating with 1300 grooves/mm blazed at 5500  $\text{\AA}$  was applied, yielding at the exit focal plane of the spectrometer reciprocal dispersions of 0.060 and 0.067  $\text{\AA}/\text{pixel}$  for the nitrogen multiplet and  $H_{\beta}$  line respectively. Suitable filters (9) were placed in front of the entrance slit (see Fig. 1) in order to block the radiation below  $\lambda = 3250$   $\text{\AA}$  and  $\lambda = 6000$   $\text{\AA}$  for measurements of the  $H_{\beta}$  and NI multiplet respectively. In this way we avoid possible interference of higher diffraction orders on the measured spectra around the  $H_{\beta}$  and the studied NI spectrum.

The technique of self-absorption checks of the plasma applied in this work is described in detail e.g. in our previous paper [10]. The radiation emerging from the plasma column in the direction opposite to the spectrometer was reflected back by the concave mirror (3) forming an arc image in its own volume and thus almost doubling the measured intensities — see Figure 1. Comparison of spectra recorded with and without back-reflection confirms that self-absorption of radiation was negligibly even for the strongest lines of interest (spectral intensities reached only 0.8% of the Planck function value at the plasma temperature). The measured light outputs from the arc were calibrated against corresponding signals measured from a tungsten strip radiation standard (2). For each studied plasma layer and arc current at least three independent expositions of the OMA analyzer have been performed. Then the corresponding spectra were averaged. In further steps of the data reduction we have worked out these averaged spectra.

At our plasma conditions the Stark effect is the dominant broadening process, however other line-broadening mechanisms must be also considered. In our case these are the instrumental and the Doppler broadening. The apparatus profile was determined applying a low-pressure discharge in hydrogen of a Plücker type. The shape of the apparatus profile could be well approximated by a Gaussian profile and its full width at half maximum was measured to be 0.12  $\text{\AA}$ . The Plücker tube ran in krypton was used also as standard source for wavelength calibration of the measured spectra.

### 2.2 Plasma diagnostics

For determination of Stark-broadening parameters the knowledge of the temperature and electron density is necessary.

The electron temperature was determined by applying the Boltzmann plot method from intensity ratios of two NI lines: one of the fine structure being studied at 7915.42  $\text{\AA}$  and the NI spectral transition at 8680.28  $\text{\AA}$ . The excitation energy gap of these lines is 2.16 eV, which is sufficient for evaluation of plasma temperatures of the order of 1 eV. The atomic transition probability data of Wiese et al. [8] were used for evaluation of the temperature. In this way for different arc currents and various selected plasma layers, temperatures from the range between 9200 and 13600 K have been determined. For this temperature interval the corresponding Doppler widths

(full-widths at half maximum) are of the order of 0.2 Å for the studied NI multiplet and 0.3 Å for the  $H_\beta$  line. We assumed that the gas temperature is nearly the same as the electron (excitation) temperature. Such assumption is justified for arc discharges at atmospheric pressure. The uncertainty of our temperature determination we estimate to be about  $\pm 800$  K.

The electron density ( $N_e$ ) was obtained by determining the Stark widths of the hydrogen  $H_\beta$  line. The contributions originating from Doppler and instrumental broadening have been subtracted from directly measured FWHM of this line. For  $N_e$  evaluations the theoretical broadening data of Gigoso and Cardenoso [11] were applied. In this manner electron densities for different arc currents and selected plasma layers from  $1.2 \times 10^{16}$  to  $2.1 \times 10^{16}$  cm $^{-3}$  have been determined. This standard spectroscopic method of electron density determination yields results for which the typical uncertainty limits do not exceed 10 percent.

### 3 Analysis of the spectra and data reduction

The aim of this paper was to provide experimental data on Stark-broadening of the NI  $3s^2D - 3p^2P^o$  multiplet. As an example, in Figure 2a we present the studied NI spectrum in the wavelength range 7880–7940 Å, together with the corresponding reference signal from the standard source. From both measured light outputs only the dark currents have been subtracted. Two of the NI fine structure components are very close in wavelength (the distance between them is only 0.3 Å) and thus they appear as a single spectral feature. As can be seen, the studied multiplet shape and the standard source spectrum are superimposed by a significant and regular interference pattern with amplitude proportional to the light intensity. In order to release the spectrum from this interference pattern, the directly recorded spectra were filtered applying the Fourier transform technique. The details of the procedure are described in [9]. The resulting smoothed spectrum is shown in Figure 2b. After applying the smoothing procedure the measured arc signals were calibrated against the corresponding light outputs of the standard source.

In Figure 2c the spectrum taken after closing the nitrogen supply into the discharge volume is shown. The recordings shown in Figures 2a and 2c are presented in the same intensity scale. In Figure 2c the nitrogen multiplet appears only as a very weak feature due to remnants of nitrogen in the arc. Besides the weak NI lines, two narrow argon transitions at wavelengths 7891.077 and 7935.8 Å appear in the spectrum, due to traces of argon in the arc regions close to both electrodes. The line at 7935.8 Å originates definitely from argon — the line has been detected also in our Plücker tube run in argon atmosphere. However this line is not listed in any argon wavelength tables available to us. Close to the classified ArI line ( $\lambda = 7891.077$  Å) an unidentified transition at  $\lambda = 7886.2$  Å appears. The comparison of spectra measured with and without nitrogen supply clearly shows that the wavelength positions

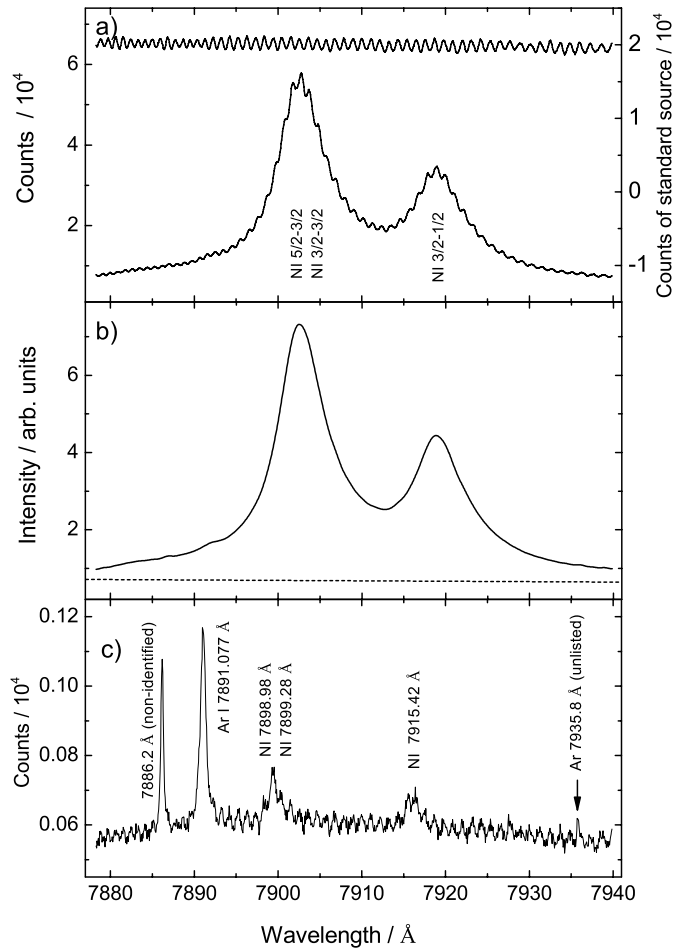


**Fig. 2.** An example of our spectral recordings for studies of the NI multiplet, illustrating the reduction of experimental data: (a) directly measured signals from the arc discharge and from the radiometric standard source (upper trace). The fractions listed below the two broaden peaks are the corresponding total momentum quantum numbers  $J_l - J_u$ , characterizing the individual fine structure components. (b) The NI spectrum calibrated against the standard source signal and after applying the smoothing procedure (Fourier transform technique). The dashed line represents the continuum level. (c) The spectrum in the same wavelength range recorded after blocking the nitrogen gas supply into the arc (displayed in the same intensity units as in part a). Except the declining NI transitions three weak disturbing lines appear — two ArI lines and one unidentified transition. For details see the text.

of the NI lines differ significantly. This observation indicates that the main contribution to the electron density originates from ionization of nitrogen atoms in the helium plasma environment. The shifts of nitrogen transitions (also of the impurity lines) are usually of the order of the half-widths of the lines. At higher electron density conditions these impurity lines are expected to be much broader and thus — though very weak in comparison to the nitrogen multiplet — they may cause an enhancement of the blue wing of the studied NI multiplet.

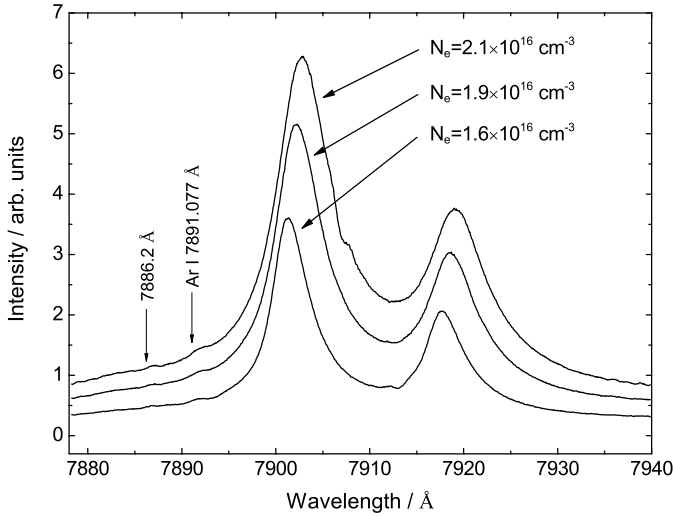


**Fig. 3.** Measured profiles of the NI multiplet at three different electron densities. Clearly seen are the trends of the broadening, shift and asymmetry of the studied spectrum. The two arrows are marking the non-shifted positions of the two disturbing lines on the blue wing of the studied multiplet.

As above mentioned our NI multiplet shape studies have been performed at different plasma conditions. Three selected profiles recorded at different electron densities and temperatures, after applying the smoothing procedure, are compared in Figure 3. As can be seen the observed line profiles are significantly broadened and exhibit large shifts increasing with growing electron density. Very strong asymmetry, which decreases slightly with increasing electron density, is also apparent. The non-shifted positions of two lines on the blue wing of the NI multiplet are marked with two arrows. The Stark-broadening, shift and asymmetry parameters of the ArI transition at wavelength 7891.077 Å are listed in Griem's monograph [1]. For our experimental conditions the shifts of this line are expected to be between 0.39 and 0.66 Å, while the FWHM are from 1.3 to 2.5 Å for the lowest and highest electron density respectively.

#### 4 Description of theoretical background and the fitting procedure

The line profiles are primarily broadened by collision with fast moving electrons. These interactions lead to shifted Lorentzian-like line shapes. Nevertheless, in the case of non-hydrogenic isolated neutral atom lines, the broadening caused by interactions with ions is not negligible. Collisions with ions lead to some additional broadening and cause an asymmetry of the profile, enhancing the line wing which complies with the shift direction. These asymmetrical profiles can be described by an asymmetric function of the  $j(x)$  type, introduced by Griem et al. [12] for description of helium line shapes. Later this approach was used by Griem [13] to calculate spectral line shapes for few other elements. The  $j(x)$  function depends on the reduced

wavelength unit ( $x$ ) as:

$$j_l(x) = \frac{1}{\pi} \int_0^\infty \frac{W_\rho(\beta) d\beta}{1 + (x - A^{4/3}\beta^2)^2}. \quad (1)$$

Here  $x$  is the reduced wavelength, and is given by:

$$x = \frac{\lambda - \lambda_l - d_e}{w_e}, \quad (2)$$

where  $\lambda$  is the wavelength,  $\lambda_l$  is the wavelength of the unperturbed fine structure component,  $d_e$  is the electron impact shift and  $w_e$  is electron impact width (half-half width). The ion broadening parameter ( $A$ ) is defined e.g. in [1], assuming that the splitting into sublevels with different magnetic quantum numbers is negligibly small. From this definition follows that  $A$  is proportional to  $N_e^{1/4}$ . The function  $W_\rho(\beta)$  is the probability density for the electric microfield of the plasma in reduced field strength scale  $\beta = F/F_0$ , where  $F_0 = e_0/R_0^2$  is the Holtzmark normal field strength and  $R_0$  is the distance defined by the relationship  $(4/15)(2\pi)^{3/2}R_0^3N_e = 1$ , which is approximately equal to the inter-ionic distance in the plasma. The parameter  $\rho$  is defined as the ratio  $\rho = R_0/D = 6^{1/3}\pi^{1/6}e_0N_e^{1/6}(kT)^{-1/2}$ , where  $D$  is electronic Debye radius. At our experimental conditions the density of ions with a charge  $Q \geq +2e$  is negligibly small in comparison to the density of singly ionized atoms. Therefore in our calculations we used the function  $W_\rho(\beta)$  at a neutral point (in the plasma) produced by singly charged perturbers and for  $\beta$  in the range  $0 \leq \beta \leq 51$ , evaluated by Halenka [15].

Under our experimental conditions the contributions from the instrumental and Doppler broadening to the resulting line widths are not negligible. The instrumental and Doppler corrections are typical of the order of 2.5% of the measured FWHM for the higher, and 6% for the lower electron density conditions. As already mentioned the instrumental profile could be well approximated with a Gaussian profile, with the FWHM  $\Delta\lambda_{1/2}^i$ . As well-known, the Doppler broadening is also described by a Gaussian profile with the Doppler width of  $\Delta\lambda_D = (\lambda_l/c)\sqrt{2kT/m}$  (all symbols are conventional). In this case the convolution of instrumental and Doppler broadening leads also to a Gaussian shape, which in the reduced wavelength scale  $x$  is given by:

$$P(x) = \frac{1}{\sqrt{\pi}} \frac{w_e}{\Delta\lambda_c} \exp(-((w_e x + d_e)/\Delta\lambda_c)^2), \quad (3)$$

where

$$\Delta\lambda_c = \sqrt{(\Delta\lambda_{1/2}^i/2\sqrt{\ln 2})^2 + (\Delta\lambda_D)^2} \quad (4)$$

is the half width of the profile  $P(x)$  on the height  $1/e$  of its maximum.

In order to determine the Stark-parameters (broadening, shift and asymmetry) characterizing the shape of the individual fine structure component, we have assumed that the electron broadening ( $w_e$ ), the electron impact-shift ( $d_e$ ) as well as the asymmetry parameters ( $A$ ) are the same for all three components. The non-shifted wavelengths in equation (2) ( $\lambda_1 = 7898.98$  Å,  $\lambda_2 = 7899.28$  Å,

and  $\lambda_3 = 7915.42 \text{ \AA}$ ) and the intensity fractions of the individual fine structure components ( $I_1 = 0.599I_0$ ,  $I_2 = 0.069I_0$ ,  $I_3 = 0.332I_0$ ), with  $I_0$  being the multiplet intensity factor, have been taken from [8]. The intensity of the continuum has been approximated by a linear function  $I_c = ax + b$ . At the above assumptions, the measured intensity was approximated by the following function:

$$J(x) = I_0 \sum_l^{term} I_l j_l(x') P_l(x - x') + ax + b. \quad (5)$$

Each experimental spectrum (for fixed  $N_e$  and  $T$ ) has been fitted by the above described function. The free fitting parameters were:

- the Stark shape characteristics  $w_e$ ,  $d_e$ ,  $A$ ;
- two parameters for the description of the continuum  $a$  and  $b$ ;
- the multiplet intensity factor  $I_0$ .

## 5 Results and discussion

In Figure 4, we present the results of our fitting procedure for one selected plasma condition  $N_e = 2.0 \times 10^{16} \text{ cm}^{-3}$ ,  $T = 13000 \text{ K}$ . In the upper part (a) of this figure the experimental data (solid line) are compared with the resulting theoretical profile of the whole multiplet (short-dash line). The dashed line on the bottom represents the continuum level. Similarly as in Figure 3, the non-shifted wavelength positions of the two disturbing lines appearing on the blue wing of the NI transition are shown. As above mentioned the expected shift of the ArI transition at this particular plasma condition is about  $0.7 \text{ \AA}$ , i.e. significantly less than the shift of the studied NI multiplet. The FWHM of the ArI line is expected to be about  $2 \text{ \AA}$ . The disagreement between the fitted profile and the experimental results on the blue wing may be, at least partly, caused by the contribution originating from these two broad transitions. In Figure 4b the profiles of the three individual fine structure components, after subtraction of the background continuum, are shown.

According to the Stark-broadening theory the electron broadening parameter ( $w_e$ ) and the electron-impact shift ( $d_e$ ) are linear functions of the electron density of the plasma. In Figure 5, we plot these two fitting parameters obtained from the analysis of all our experimental data. The rather weak scatter of the measuring points seems to confirm the correctness of our fitting procedure. The determined electron impact widths are in the range from about 1.4 to 2.9, i.e. correspond satisfactorily with the electron density range ( $1.2 \times 10^{16} \div 2.1 \times 10^{16} \text{ cm}^{-3}$ ) obtained from our diagnostic procedure based on measurements of the FWHM of the  $H_\beta$  transition. The ratios between the respective boundary values are 2.07 and 1.75. This disagreement is not surprising since the electron impact width increases somewhat with raising temperature. In the case of our plasma source higher temperature conditions correspond to higher  $N_e$ -values. On the other hand the electron-impact shifts are in the range from 0.8 to 2.7,

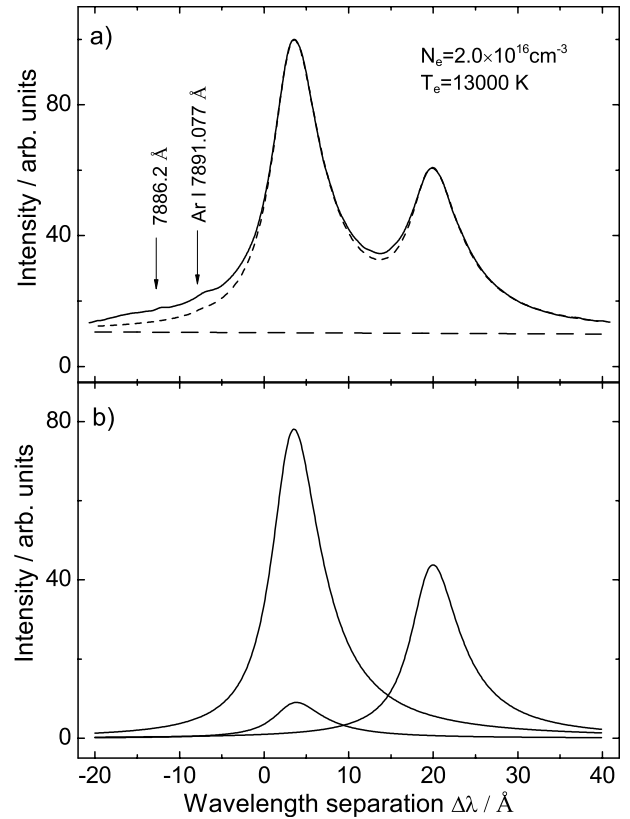


**Fig. 4.** Comparison of measured and fitted NI profiles at the following plasma conditions:  $N_e = 2 \times 10^{16} \text{ cm}^{-3}$  and  $T = 13000 \text{ K}$ : (a) comparison of the measured (solid line) and the fitted profile (short-dash line). The dashed line represents the continuum level, while the arrows are showing the non-shifted positions of the disturbing lines, (b) the fitted profile decomposed into the three fine structure components, after subtracting the continuum background.

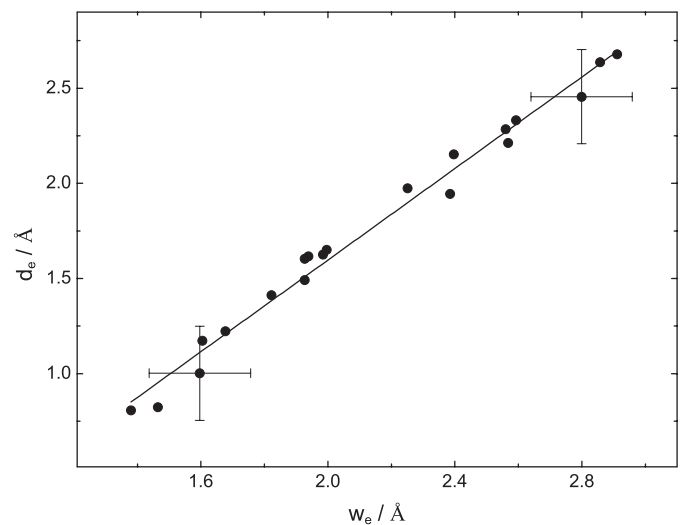


**Fig. 5.** The plot of two fitting parameters — the electron impact-shift ( $d_e$ ) versus the electron impact-width ( $w_e$ ), indicating similar dependence on our main plasma conditions  $N_e$  and  $T$ .

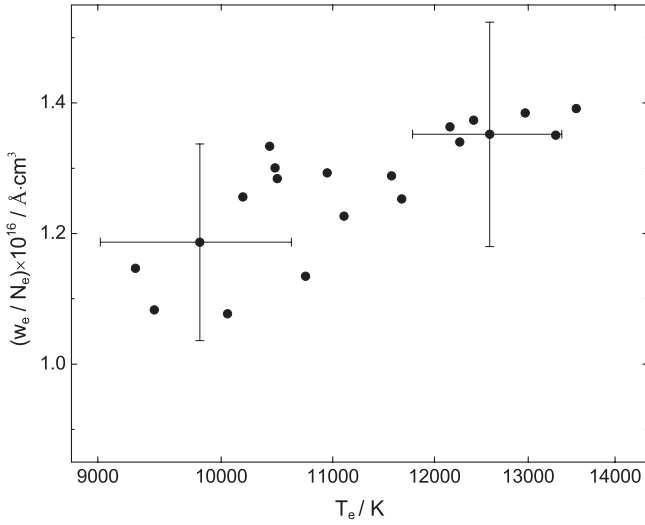


**Fig. 6.** The normalized (to the standard electron density value of  $N_e = 10^{16} \text{ cm}^{-3}$ ) electron impact widths (linear scale) as a function of the plasma temperature (logarithmic scale). The vertical error bars are obtained by taking into account the uncertainties of electron density determination. A clear trend is apparent — the normalized electron impact width increases with increasing temperature.

i.e. exceeding significantly the range expected from the  $N_e$  interval, indicating that the electron impact-shift depends strongly on temperature. Detailed analysis of the uncertainty of our measurements and fitting procedure, performed on the basis of individually recorded spectra at the same plasma conditions, reveals that the scatter of the parameters  $d_e$  and  $A$  was systematically larger than for the parameter  $w_e$ . Standard deviations of individual measurements were calculated. These standard deviations averaged over the whole set of fitting results  $\langle \Delta x_{i,st}/x_i \rangle_n$  are equal to 5%, 11% and 15% for the parameters  $w_e$ ,  $d_e$  and  $A$ , respectively. Therefore our electron impact-shifts and asymmetry results have to be regarded as being less reliable as our data concerning the broadening parameter. One possible reason of this larger uncertainty is that the asymmetry parameter ( $A$ ) contribute to the evaluated line width as well as to the total line shift and thus the statistical uncertainty of the determination of this parameter may influence the respective uncertainties of the  $w_e$  and  $d_e$  determination.

As above-mentioned the asymmetry parameter ( $A$ ) scales with the electron density of the plasma as  $N_e^{1/4}$ , while the other parameters — the electron impact width ( $w_e$ ) and the electron impact-shift ( $d_e$ ) depend linearly on  $N_e$ . In order to compare our experimental data, determined at different electron densities, we have reduced our results to the so-called normalized (standard) electron density of  $10^{16} \text{ cm}^{-3}$ . In Figure 6 the normalized electron impact widths ( $w_e$ ) are plotted (in semi-logarithmic scale) against the temperature of the plasma. A clear tendency is apparent — the width is increasing with the plasma temperature. In Figure 7 the normalized  $d_e$  and  $A$  fitting

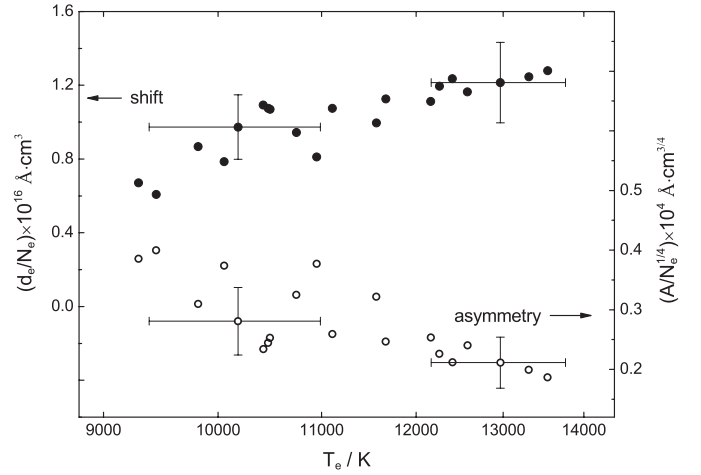


**Fig. 7.** The normalized (to the standard electron density value of  $N_e = 10^{16} \text{ cm}^{-3}$ ) electron impact shifts (left-hand linear scale) and asymmetry parameters (right-hand linear scale), both versus the plasma temperature (logarithmic scale). The vertical error bars are obtained by taking into account the uncertainties of electron density determination. With respect to temperature dependence the two Stark-broadening parameters  $d_e$  and  $A$  clearly show opposite trends. The characteristic scatter of the measuring points indicates that fittings of similar quality may be obtained for different pairs of these two fitting parameters.

parameters are shown as a function of the temperature of the plasma, again in semi-logarithmic scale. The electron impact-shift slightly increases, while the asymmetry parameter decreases with increasing  $N_e$ . Both observations are not surprising since such behavior is rather typical for isolated NI transitions quoted in [1]. In the last two figures (Figs. 6 and 7) typical error bars are shown for always two measuring points. The uncertainty of normalized  $w_e$  values does not exceed 13%, but the uncertainties of the  $d_e$  and  $A$  parameters are larger reaching about 20%.

## 6 Conclusions

Stark-broadening parameters: electron impact widths ( $w_e$ ), electron impact shifts ( $d_e$ ) and asymmetry parameters ( $A$ ) of fine structure components of the NI multiplet ( $^1\text{D}$ ) $3s \ ^2\text{D} - (^1\text{D})3p \ ^2\text{P}^o$  have been experimentally determined. Measurements have been performed at electron densities of the plasma varying from  $N_e = 1.2 \times 10^{16} \text{ cm}^{-3}$  to  $N_e = 2.1 \times 10^{16} \text{ cm}^{-3}$ , applying an arc discharge in a helium-nitrogen mixture. The main plasma parameters, crucial for the interpretation of the measured broadening data of the NI multiplet — the electron density and temperature of the plasma, have been obtained applying standard spectroscopical techniques ( $\text{H}_\beta$  broadening, Boltzmann plot method). The studied NI multiplet exhibits anomalous strong broadening, shift and asymmetry if compared to majority of NI transitions in the visible and ultraviolet part of the spectrum.

## References

1. H.R. Griem, *Spectral line broadening by plasmas* (Academic Press, New York, 1974)
2. H.R. Griem, *Plasma spectroscopy* (McGraw-Hill, New York, 1964)
3. J. Barnard, J. Cooper, E.W. Smith, *J. Quant. Spectrosc. Radiat. Transfer* **14**, 1025 (1974)
4. J.M. Bassalo, M. Cattani, V.S. Walder, *J. Quant. Spectrosc. Radiat. Transfer* **28**, 75 (1982)
5. M.S. Dimitrijević, S. Sahal-Brechot, *Astron. Astrophys. Suppl. Ser.* **82**, 519 (1990); *Bull. Obs. Astron. Belgrade* **141**, 57 (1989)
6. J. Musielok, *J. Tech. Phys. Suppl.* **40**, 259 (1999)
7. T. Wujec, J. Halenka, A. Jazgara, J. Musielok, *J. Quant. Spectrosc. Radiat. Transfer* **74**, 663 (2002)
8. W.L. Wiese, J.R. Fuhr, T.M. Deters, *Atomic transition probabilities of carbon, nitrogen and oxygen: a critical data compilation* (*J. Phys. Chem. Ref. Data, Monograph* **7**, 1996)
9. T. Wujec, W. Olchawa, J. Halenka, J. Musielok, *Phys. Rev. E* **66**, 066403 (2002)
10. T. Wujec, A. Baćłowski, A. Golly, I. Książek, *Acta Phys. Pol. A* **96**, 333 (1999)
11. M.A. Gigoso, V. Cardenoso, *J. Phys. B* **29**, 4795 (1996)
12. H.R. Griem, M. Baranger, A.C. Kolb, G.K. Oertel, *Phys. Rev.* **125**, 177 (1962)
13. H.R. Griem, *Phys. Rev.* **128**, 515 (1962)
14. W.C. Martin, W.L. Wiese, *Atomic Spectroscopy*, in *Atomic, Molecular and Optical Physics Handbook*, edited by G. Drake (Am. Inst. of Physics, Woodbury, New York, 1966)
15. <http://draco.uni.opole.pl/Halenka.html>